Estimation of Synchronization Errors between Master and Slave Chaotic Systems with Matched/Mismatched Disturbances and Input Uncertainty

Chih-Hsueh Lin [1], Guo-Hsin Hu [1,2] and Jun-Juh Yan [3,*]

[1] Department of Electronic Engineering, National Kaohsiung University of Science and Technology, Kaohsiung 80778, Taiwan; cslin@nkust.edu.tw (C.-H.L.); guohsin@mail.mirdc.org.tw (G.-H.H.)

[2] Department of Industrial Upgrading Service, Metal Industries Research & Development Centre, Kaohsiung 81160, Taiwan

[3] Department of Electronic Engineering, National Chin-Yi University of Technology, Taichung 41107, Taiwan

[*] Correspondence: jjyan@ncut.edu.tw

Abstract: This study is concerned with robust synchronization for master–slave chaotic systems with matched/mismatched disturbances and uncertainty in the control input. A robust sliding mode control (SMC) is presented to achieve chaos synchronization even under the influence of matched/mismatched disturbances and uncertainty of inputs. A proportional-integral (PI) switching surface is introduced to make the controlled error dynamics in the sliding manifold easy to analyze. Furthermore, by using the proposed SMC scheme even subjected to input uncertainty, we can force the trajectories of the error dynamics to enter the sliding manifold and fully synchronize the master–slave systems in spite of matched uncertainties and input nonlinearity. As for the mismatched disturbances, the bounds of synchronization errors can be well estimated by introducing the limit of the Riemann sum, which is not well addressed in previous works. Simulation experiments including matched and mismatched cases are presented to illustrate the robustness and synchronization performance with the proposed SMC synchronization controller.

Keywords: chaos synchronization; sliding mode control; mismatched disturbance; Riemann sum

1. Introduction

Chaotic phenomena exist frequently in many nonlinear engineering systems; the chaos dynamic behavior is unstable but bounded and contains infinite non-periodic trajectories in strange attractors. In particular, its state response is very sensitive to the initial values of states, and this is the well-known butterfly effect. Owing to its distinguished advantages in various research fields, chaos control and synchronization has increasingly received attention [1,2]. Particularly, its application to communication security is one of the most important topics in the research of chaos synchronization. By realizing chaos synchronization, the communication system can simultaneously obtain dynamical and random chaotic numbers at the transmitting and receiving ends, and then it becomes possible to further design the chaotic ciphers [3]. Hence, many different synchronization control approaches have been reported in the literature, such as time-varying delay feedback control [4], sliding mode control [5–7], linear state feedback control [8], fuzzy sliding mode control [9–11], H-infinity stabilization [12,13] and adaptive control [14,15]. For controlled systems, there always exist unknown external perturbations or uncertainties, including unmodeled system dynamics and control input uncertainty due to the component nonlinearities and external disturbances. These disturbances often cause degradation or even failure of the control performance. Therefore, designing a robust control scheme to asymptotically suppress or eliminate the influence of unknown disturbances is a very important issue when discussing synchronization control for chaotic systems [16], and some research works

have been proposed by studying the effects of input uncertainties [17–19]. By considering the uncertainties for control inputs, the state synchronization controller for two identical n-dimensional chaotic systems was proposed in [17], and the robust adaptive finite-time controller was reported for synchronization in [18]. For second-order chaotic systems, the synchronization controller was proposed by the adaptive sliding mode control [19]. To design a control system, sliding mode control (SMC) is an outstanding method due to the good transient performance, fast response and the robustness to uncertain system parameters or external disturbances, especially when the matching condition is satisfied [20,21]. By surveying the above-mentioned papers, it was found that the works [2–4,6,8,15,20] only considered some special classes of chaotic systems, and the unavoidable uncertainty in control input was not considered. The reports in [5–7,11,21] introduced the SMC approach to achieve robust synchronization. However, the perturbations of parameters were often considered only with the matched condition, and their approaches cannot cope with mismatched disturbances. In [12,13], the authors considered the synchronization for systems with mismatched disturbances, and the influence of mismatched disturbances was evaluated in the sense of H-infinity control. However, the uncertainty in the control input is not considered. In [17–19], researchers took into account the effects of input uncertainties for synchronization controller design. However, only special types of chaotic systems and matched disturbances were considered. Furthermore, for the case of mismatched disturbances, the individual performances for every error state between master and slave systems could not be estimated in their works.

Based on the aforementioned, we aim to discuss the design of robust SMC controllers for synchronization between master and slave chaotic systems. In comparison with the past studies mentioned above, the advantages of the proposed SMC controller are not only that it achieves synchronization for generalized classes of chaotic systems even with input uncertainty and mismatched disturbances, but also that it gives a clear evaluation of synchronization performance for every error state. Furthermore, a proportional-integral (PI) switching function is introduced to avoid the reduced-order property in the traditional SMC such that it becomes easy to estimate the synchronization performance between master–slave systems in sliding manifold for mismatched disturbances. This proposed SMC can always drive the trajectories of the controlled dynamics to hit and enter the sliding mode and fully synchronize the master–slave systems in spite of matched uncertainties and input nonlinearity. As for the mismatched disturbances, the bounds of synchronization errors can be well estimated by utilizing the limit of the Riemann sum. Two simulation experiments including matched and mismatched cases are given to demonstrate the effectiveness of the proposed SMC design method.

Notations: I_n is the identity matrix of $n \times n$, and M^T represents the transpose for a matrix or vector. $\|x\| = \sqrt{x^T x}$ denotes the Euclidean norm of the vector $x \in R^n$. $\lambda_i(A), i = 1, 2, \ldots, n$ is the eigenvalues of matrix $A \in R^{n \times n}$. $\|A\| = \left[\lambda T_{max}[] \right]^{\frac{1}{2}}$ is the matrix norm of A. $Sign(S) = \begin{bmatrix} sign(s_1) & sign(s_2) & \ldots & sign(s_m) \end{bmatrix}^T \in R^m$ and $sign(s)$ is the sign function of s, if $s > 0$, $sign(s) = 1$; if $s = 0$, $sign(s) = 0$; if $s < 0$, $sign(s) = -1$.

2. System Definition and Problem Statement

The goal of this study is to design an SMC to solve the robust synchronization problem of master–slave chaotic systems even with mismatched disturbances and uncertainty in the control. We consider a general form in (1), which can describe many chaotic systems, such as four-dimensional generalized Lorenz–Stenflo system, the unified chaotic system, Sprott system, Rossler system, Lorenz system, Duffing oscillator, Chua's circuit, etc. A general form for master chaotic systems is described by

Master chaotic system:

$$\dot{x}_m(t) = Ax_m(t) + Bf(x_m(t), t) \tag{1}$$

and the slave chaotic system with undesired input uncertainty and matched/mismatched is described as follows.

Slave chaotic system:

$$\dot{x}_s(t) = Ax_s(t) + B(f(x_s(t),t) + \Delta f(x_s(t),t) + u(t) + \Delta u(t)) \\ + B_\omega \omega(t) \tag{2}$$

where $A \in R^{n \times n}$, $B \in R^{n \times m}$ are system matrices. The matrix pair (A, B) is controllable, meaning that the controllability matrix $R = \begin{bmatrix} B & AB & \dots & A^{n-1}B \end{bmatrix}$ has full row rank (i.e., $Rank(R) = n$). $B_\omega \in R^{n \times r}$ represents the mismatched matrix of systems, $x_m(t) \in R^n$, $x_s(t) \in R^n$, $u(t) \in R^m$, $\Delta u(t) \in R^m$, $f(x_m(t),t) \in R^m$, $f(x_s(t),t) \in R^m$, $\Delta f(x_s(t),t) \in R^m$ and $\omega(t) \in R^r$ are the state vector of master systems, the state vector of slave systems, the input vector, the unknown but bounded input perturbation, the master system nonlinear vector, the slave system nonlinear vector, the unknown but bounded nonlinear disturbance of the slave system and the mismatched disturbance vector, respectively. Besides the unknown disturbance satisfies $\Delta f(x_s(t),t) = \Delta f_1(x_s(t),t) + \Delta f_2(t)$ and is assumed to be bounded by $\|\Delta f_1(x_s(t),t)\| \le \alpha_1\|x_s(t)\|$, $\|\Delta f_2(t)\| \le \alpha_2$. The unknown $\omega(t)$ is also bounded by $\|\omega(t)\| \le \alpha_\omega$, and the input uncertainty satisfies $|\Delta u_i(t)| \le \alpha_{ui}|u_i(t)|, i = 1, 2, \dots, m$ and $\alpha_u = \max_i \alpha_{ui} < 1$.

Considering (1) and (2), we have the following error state equation.

$$\dot{e}(t) = Ae(t) + B(f(x_s(t),t) - f(x_m(t),t) + \Delta f(x_s(t),t) + u(t) \\ + \Delta u(t)) + B_\omega \omega(t) \tag{3}$$

where $e(t) = x_s(t) - x_m(t)$.

Here the control goal is to present a design procedure of SMC controller robust to bounded input uncertainty and to solve the chaos synchronization problem. To complete this synchronization controller design, two steps are included. First, it is necessary to choose an appropriate switching surface such that the error dynamics in the sliding manifold can be easily analyzed and the error bounds for matched/mismatched disturbances can be estimated. Second, a robust SMC is necessary to guarantee the hitting condition and keep the system trajectories in the sliding manifold even under the influence of input uncertainty. In the following section, we will discuss the designs of a switching surface and robust SMC controller.

3. Switching Surface Design and Performance Estimation in the Sliding Manifold

To complete the above design steps, we first introduce a PI sliding surface that can avoid the reduce order property in the traditional SMC and make it easy to estimate and analyze the error dynamics when the controlled system is driven to the sliding manifold. We choose the PI switching surface, which is defined as follows

$$S(t) = \sigma e(t) - \int_0^t (\sigma A - K)e(\tau)d\tau \tag{4}$$

where $\sigma = B^\dagger = (B^T B)^{-1} B^T$ is the generalized inverse satisfying $\sigma B = I_m$, K is the control gain matrix selected such that the eigenvalues $\lambda_i, i = 1, 2, \dots, n$ of matrix $(A - BK)$ are different real numbers and satisfy $\lambda_i < 0, i = 1, 2, \dots, n$.

Differentiating (4), we obtain

$$\dot{S}(t) = \sigma(Ae(t) + B(f(x_s(t),t) - f(x_m(t),t) + \Delta f(x_s(t),t) + u(t) + \Delta u(t)) + B_\omega \omega(t)) \\ - \sigma Ae(t) + Ke(t) \tag{5}$$

Assume the system is in the sliding manifold for $t \ge t_s$ (t_s is the hitting time), i.e., $S(t) = 0$ and $\dot{S}(t) = 0$, the equivalent control $u_{eq}(t)$ can be obtained from (5) with $\dot{S}(t) = 0$ as

$$u_{eq}(t) = -f(x_s(t), t) + f(x_m(t), t) - \Delta f(x_s(t), t) - \Delta u(t)$$
$$-\sigma B_\omega \omega(t) - Ke(t) \tag{6}$$

Substituting (6) into (3), we can have the synchronization error dynamics in the sliding manifold as

$$\dot{e}(t) = \widetilde{A}e(t) + \widetilde{\omega}(t) \tag{7}$$

where $\widetilde{A} = A - BK, \widetilde{\omega}(t) = (I - B\sigma)B_\omega \omega(t)$.

As is well known, since matrix pair (A, B) is controllable, we can easily obtain a specified matrix K by using the pole assignment approach such that all eigenvalues of $\widetilde{A} = A - BK$ satisfy $\lambda_i(A - BK) < 0, i = 1, 2, \ldots, n$. Solving (7), one has the solution of $e(t)$ for $t \geq t_s$ (t_s is the hitting time) as

$$e(t) = e^{\widetilde{A}(t - t_s)}e(t_s) + \int_{t_s}^{t} e^{\widetilde{A}(t - \tau)}\widetilde{\omega}(\tau)d\tau \tag{8}$$

Next, selecting a matrix $P = \begin{bmatrix} p_1 & p_2 & \cdots & p_n \end{bmatrix} \in R^{n \times n}$ to transform the matrix $\widetilde{A}$ to be diagonal and satisfy $P^{-1}\widetilde{A}P = \Lambda, \Lambda = diag(\lambda_1, \lambda_2, \ldots, \lambda_n)$, where $p_i \in R^{n \times 1}$ is the independent eigenvector corresponding to eigenvalue λ_i of matrix $\widetilde{A}$.

From (8), by introducing the fact of $e^{\widetilde{A}t} = Pe^{\Lambda t}P^{-1}$, one has

$$e(t) = Pe^{\Lambda(t - t_s)}P^{-1}e(t_s) + \int_{t_s}^{t} Pe^{\Lambda(t - \tau)}P^{-1}\widetilde{\omega}(\tau)d\tau \tag{9}$$

The solution of every $e_i(t), i = 1, 2, \ldots, n$ can be individually obtained as

$$e_i(t) = \phi_i e(t)$$
$$= \phi_i Pe^{\Lambda(t - t_s)}P^{-1}e(t_s) + \phi_i \int_{t_s}^{t} Pe^{\Lambda(t - \tau)}P^{-1}\widetilde{\omega}(\tau)d\tau \tag{10}$$
$$= \phi_i Pe^{\Lambda(t - t_s)}P^{-1}e(t_s) + \phi_i \int_{t_s}^{t} Pe^{\Lambda(t - \tau)}P^{-1}(I - B\sigma)B_\omega \omega(\tau)d\tau$$

where ϕ_i is i-row of I_n.

According to (10), we have

$$|e_i(t)| \leq \left| \phi_i Pe^{\Lambda(t - t_s)}P^{-1}e(t_s) \right| + \left| \phi_i \int_{t_s}^{t} Pe^{\Lambda(t - \tau)}P^{-1}(I - B\sigma)B_\omega \omega(\tau)d\tau \right| \tag{11}$$

Next, introducing the limit of the Riemann sum [22], the term of $\phi_i \int_{t_s}^{t} Pe^{\Lambda(t - \tau)}P^{-1}$ $(I - B\sigma)B_\omega \omega(\tau)d\tau$ in (11) can be described as below

$$\phi_i \int_{t_s}^{t} Pe^{\Lambda(t - \tau)}P^{-1}(I - B\sigma)B_\omega \omega(\tau)d\tau = \phi_i \lim_{n \to \infty} \sum_{j=1}^{n} Pe^{\Lambda(t - t^*)}P^{-1}(I - B\sigma)B_\omega \omega(t^*)\Delta\tau \tag{12}$$

where $\Delta\tau = \frac{t - t_s}{n} > 0, n \to \infty$ and $t^* = t_s + \Delta\tau \cdot j$. Thus, we have

$$\left| \phi_i \int_{t_s}^{t} Pe^{\Lambda(t - \tau)}P^{-1}(I - B\sigma)B_\omega \omega(\tau)d\tau \right|$$
$$= \left| \phi_i \lim_{n \to \infty} \sum_{j=1}^{n} Pe^{\Lambda(t - t^*)}P^{-1}(I - B\sigma)B_\omega \omega(t^*)\Delta\tau \right|$$
$$= \left| \phi_i P(\lim_{n \to \infty} \sum_{j=1}^{n} e^{\Lambda(t - t^*)}\Delta\tau)P^{-1}(I - B\sigma)B_\omega \omega(t^*) \right| \tag{13}$$
$$\leq \|\phi_i P(\lim_{n \to \infty} \sum_{j=1}^{n} e^{\Lambda(t - t^*)}\Delta\tau)P^{-1}(I - B\sigma)B_\omega\| \|\omega(t^*)\|$$
$$\leq \|\phi_i P \int_{t_s}^{t} e^{\Lambda(t - \tau)}d\tau P^{-1}(I - B\sigma)B_\omega\| \max_{t \geq t_s}\|w(t)\|$$

By substituting (13) into (11), the bound of every $e_i(t), i = 1, 2, \ldots, n$ for $t \geq t_s$ can be estimated by

$$|e_i(t)| \leq \left| \phi_i P e^{\Lambda(t-t_s)} P^{-1} e(t_s) \right|$$

$$+ \left\| \phi_i P \int_{t_s}^t e^{\Lambda(t-\tau)} d\tau P^{-1} (I - B\sigma) B_\omega \right\| \max_{t \geq t_s} \|w(t)\| \tag{14}$$

$$\leq \left| \phi_i P e^{\Lambda(t-t_s)} P^{-1} e(t_s) \right| + \alpha_w \left\| \phi_i P \cdot diag\left(\frac{-1}{\lambda_1} + \frac{e^{\lambda_1(t-t_s)}}{\lambda_1}, \ldots, \frac{-1}{\lambda_n} + \frac{e^{\lambda_n(t-t_s)}}{\lambda_n} \right) P^{-1} (I - B\sigma) B_\omega \right\|$$

Since $\lambda_i < 0$ is specified, we can estimate the bounds ρ_i of $e_i(t)$ as

$$\begin{aligned}
\rho_i &= \lim_{t \to \infty} |e_i(t)| \\
&\leq \lim_{t \to \infty} \left| \phi_i P e^{\Lambda(t-t_s)} P^{-1} e(t_s) \right| \\
&\quad + \lim_{t \to \infty} \alpha_w \left\| \phi_i P \cdot diag\left(\frac{-1}{\lambda_1} + \frac{e^{\lambda_1(t-t_s)}}{\lambda_1}, \ldots, \frac{-1}{\lambda_n} + \frac{e^{\lambda_n(t-t_s)}}{\lambda_n} \right) P^{-1} (I - B\sigma) B_\omega \right\| \\
&\leq \alpha_w \left\| \phi_i P \cdot diag\left(\frac{-1}{\lambda_1}, \ldots, \frac{-1}{\lambda_n} \right) P^{-1} (I - B\sigma) B_\omega \right\|
\end{aligned} \tag{15}$$

Remark 1. *If the uncertain slave system (2) is only subjected to matched uncertainties (i.e., the matrix B_ω can be represented as $B_\omega = BB_1$ for some matrix B_1), then we have $(I - B\sigma)B_\omega = 0$. According to (15), one can conclude that when the controlled system is with matched uncertainties and disturbances, the synchronization errors can fully converge to zero, i.e., $\rho_i = 0, i = 1, 2, \ldots, n$.*

From above discussion, we can estimate the individual bound of synchronization errors in the sliding manifold for matched/mismatched disturbances. However, the bounds are obtained for the systems in the sliding manifold. Therefore, we still need to propose an SMC controller robust to input uncertainty to guarantee the sliding motion of $S(t) = 0$.

4. Robust SMC Controller Design

Before continuing the SMC controller design, the following hitting condition based on the Lyapunov stability theorem is presented to ensure the existence of the sliding manifold.

Lemma 1. *The trajectory of the error dynamics (3) always converges to the sliding surface $S(t) = 0$, if the following hitting condition is satisfied*

$$S^T(t)\dot{S}(t) < 0 \tag{16}$$

Proof. According to Lyapunov stability theory, we select a Lyapunov function $V(t) = 0.5S^T(t)S(t) > 0$ for all $S(t) \neq 0$. Obviously, condition (16) implies that $\dot{V}(t) = S^T(t)\dot{S}(t) < 0$. Therefore, $V(t)$ as well as the switching function $S(t)$ can converge to zero.

For satisfying the hitting condition (16), the SMC control input subjected to bounded uncertainty is proposed as

$$u(t) = -\xi\psi(t)sign(S(t)), \quad \xi > (1 - \alpha_u)^{-1} \tag{17}$$

where $\psi(t) = \|f(x_s(t), t) - f(x_m(t), t) + Ke(t)\| + \alpha_1\|x_s(t)\| + (\alpha_2 + \alpha_\omega\|\sigma B_\omega\|)$. $\square$

Theorem 1. *Consider the uncertain error dynamics (3) with bounded input uncertainty, the system trajectory controlled by the SMC controller (17) can asymptotically converge to the sliding manifold $S(t) = 0$.*

Proof. By introducing (3) and the SMC controller (17) into $S^T(t)\dot{S}(t)$, we obtain

$$
\begin{aligned}
S^T(t)\dot{S}(t) &= S^T(t)(f(x_s(t),t) - f(x_m(t),t) + \Delta f(x_s(t),t) + u(t) + \Delta u(t) + \sigma B_\omega \omega(t)) + Ke(t) \\
&\leq \|S(t)\|(\|(f(x_s(t),t) - f(x_m(t),t) + Ke(t)\| + \alpha_1\|x_s(t)\| + (\alpha_2 + \alpha_\omega\|\sigma B_\omega\|)) \\
&\quad + S^T(t)(u(t) + \Delta u(t))
\end{aligned}
\tag{18}
$$

Since $|\Delta u_i(t)| \leq \alpha_{ui}|u_i(t)|, i = 1, 2, \ldots, m$ for the input uncertainty, we have

$$
|\Delta u_i(t)u_i(t)| = |\Delta u_i(t)||u_i(t)| \leq \alpha_{ui}|u_i(t)||u_i(t)| = \alpha_{ui}u_i^2(t)
\tag{19}
$$

From (19), we have $-\alpha_{ui}u_i^2(t) \leq \Delta u_i(t)u_i(t) \leq \alpha_{ui}u_i^2(t)$ and

$$
-\alpha_u \sum_{i=1}^{m} u_i^2(t) \leq u^T(t)\Delta u(t) = \sum_{i=1}^{m} u_i(t)\Delta u_i(t) \leq \sum_{i=1}^{m} \alpha_{ui}u_i^2(t) \leq \alpha_u \sum_{i=1}^{m} u_i^2(t)
\tag{20}
$$

Therefore, we can obtain

$$
-\alpha_u u^T(t)u(t) \leq u^T(t)\Delta u(t) \leq \alpha_u u^T(t)u(t)
\tag{21}
$$

By substituting (17) into (21), we have

$$
\begin{aligned}
-\alpha_u \xi\psi(t)sign^T(S(t))sign(S(t)) &\leq -sign^T(S(t))\Delta u(t) \leq \alpha_u \xi\psi(t)sign^T(S(t))sign(S(t)) \\
\Rightarrow -\alpha_u \xi\psi(t) \sum_{i=1}^{m} sign^2(s_i(t)) &\leq -\sum_{i=1}^{m} sign(s_i(t))\Delta u_i(t) \leq \alpha_u \xi\psi(t) \sum_{i=1}^{m} sign^2(s_i(t))
\end{aligned}
\tag{22}
$$

Multiplying $s_i^2(t)$ into (22) yields

$$
-\alpha_u \xi\psi(t) \sum_{i=1}^{m} sign^2(s_i(t))s_i^2(t) \leq -\sum_{i=1}^{m} sign(s_i(t))s_i^2(t)\Delta u_i(t) \leq \alpha_u \xi\psi(t) \sum_{i=1}^{m} sign^2(s_i(t))s_i^2(t)
\tag{23}
$$

By using the fact of $s_i(t)sign(s_i(t)) = |s_i(t)|$, we have

$$
-\alpha_u \xi\psi(t) \sum_{i=1}^{m} s_i^2(t) \leq -\sum_{i=1}^{m} |s_i(t)|s_i(t)\Delta u_i(t) \leq \alpha_u \xi\psi(t) \sum_{i=1}^{m} s_i^2(t)
\tag{24}
$$

From (24), we can conclude

$$
S^T\Delta u(t) = \sum_{i=1}^{m} s_i(t)\Delta u_i(t) \leq \alpha_u \xi\psi(t) \sum_{i=1}^{m} |s_i(t)|
\tag{25}
$$

Hence, from (18) and (25), we have

$$
\begin{aligned}
S^T(t)\dot{S}(t) &\leq \|S(t)\|\psi(t) - \xi\psi(t)S^T(t)sign(S(t)) + S^T(t)\Delta u(t) \\
&\leq \|S(t)\|\psi(t) - (1 - \alpha_u)\xi\psi(t) \sum_{i=1}^{m} |s_i(t)|
\end{aligned}
\tag{26}
$$

Furthermore, since $\|S(t)\| = \sqrt{\sum_{i=1}^{m} s_i^2(t)} \leq \sum_{i=1}^{m} |s_i(t)|$ and $\xi > (1 - \alpha_u)^{-1}$ are selected, we have

$$
S^T(t)\dot{S}(t) \leq \psi(t) \sum_{i=1}^{m} |s_i(t)| - (1 - \alpha_u)\xi\psi(t) \sum_{i=1}^{m} |s_i(t)| \leq (1 - \xi(1 - \alpha_u))\psi(t) \sum_{i=1}^{m} |s_i(t)| < 0
\tag{27}
$$

Thus, according to Lemma 1, one can conclude that the system trajectory asymptotically converges to the sliding manifold $S(t) = 0$. $\square$

Remark 2. *From the theoretical point of view, the discontinuous sign function in control input (17) may cause chattering. To reduce the chattering resulted from the discontinuous sign function, we can introduce the continuous saturation function described by*

$$sat(s_i(t)) = \frac{s_i(t)}{|s_i(t)| + \varepsilon_i},$$ (28)

where $\varepsilon_i > 0$ is sufficiently small.

Obviously, when ε_i is sufficiently small, then $sign(s_i(t))$ can be approximated by $sat(s_i(t))$ and the control input $u(t)$ can be modified as the following control law [23].

$$u(t) = -\xi\psi(t)sat(S(t))$$ (29)

where $sat(S(t)) = \left[\begin{array}{cccc} \frac{s_1(t)}{|s_1(t)|+\varepsilon_1}, & \frac{s_2(t)}{|s_2(t)|+\varepsilon_2}, & \cdots, & \frac{s_m(t)}{|s_m(t)|+\varepsilon_m} \end{array} \right]^T$.

Obviously, the continuous controller (29) with a sufficiently small value of ε_i can approach the discontinuous controller (17) very closely.

Remark 3. *According to the above discussion, we can systematize the design procedure for robust chaos synchronization as follows.*

Step 1: *Construct the master–slave systems as (1), (2) and check the controllability of matrix pair (A, B).*

Step 2: *With the controllable matrix pair (A, B), using any available pole assignment approach to calculate the gain matrix K such that the eigenvalues $\lambda_i, i = 1, 2, \ldots, n$ of matrix $\widetilde{A} = (A - BK)$ in (7) are all different and satisfy $\lambda_i < 0$, to guarantee a stable sliding manifold.*

Step 3: *construct the PI type-switching function $S(t)$ by (4).*

Step 4: *Find independent eigenvectors corresponding to eigenvalue λ_i of matrix $\widetilde{A}$ and construct the transform matrix P.*

Step 5: *According to (15), calculate the error bounds.*

Step 6: *Obtain the SMC synchronization controller from (17) or (29).*

5. Numerical Simulation Results

In this section, we give two examples to demonstrate the availability of the proposed robust SMC synchronization controller for the Sprott chaotic circuit [24] and four-dimensional generalized Lorenz–Stenflo systems [25].

Example 1. *In this example, we show that the proposed SMC controller can synchronize chaotic systems only using a single input. We consider the Sportt chaotic system [24] described by*

$$\dot{x}_1(t) = x_2(t)$$
$$\dot{x}_2(t) = x_3(t)$$ (30)
$$\dot{x}_3(t) = \beta_1 x_1(t) + \beta_2 x_2(t) - \beta_3 x_3(t) + 2\beta_4 sign(x_1(t))$$

where $x_i, i = 1, 2, 3$, are the state variables and $\beta_i, i = 1, 2, 3, 4$ are system parameters.

System (30) exhibits chaotic strange attractors, as shown in Figure 1 when $\beta_1 = -1.2$, $\beta_2 = -1$, $\beta_3 = -0.6$ and $\beta_4 = 2.8$. Obviously, we can rewrite (30) in the form of (1).
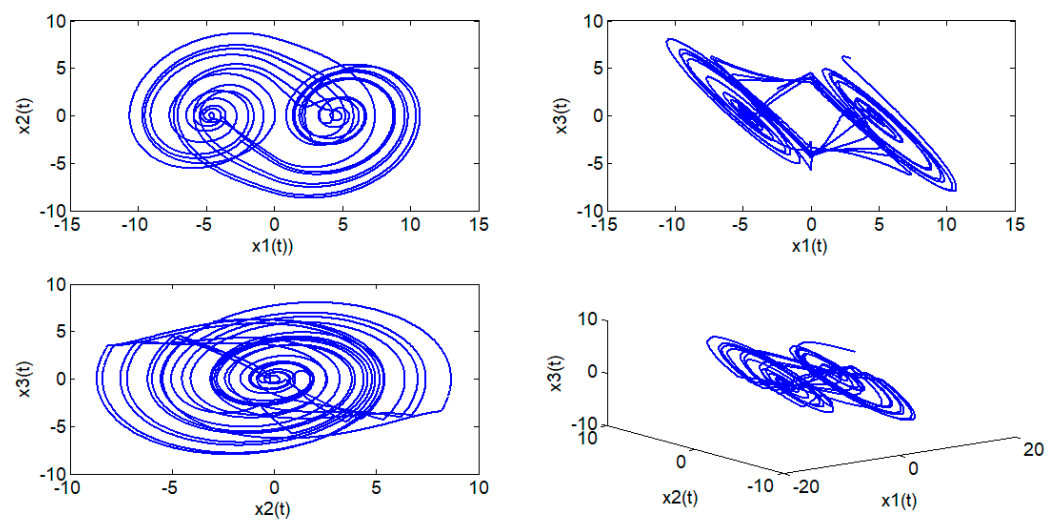
Figure 1. Strange attractors of the Sportt chaotic system.

$$\dot{x}(t) = Ax(t) + B(f(x,t)) \tag{31}$$

where $A = \begin{bmatrix} 0 & 1 & 0 \\ 0 & 0 & 1 \\ -1.2 & -1 & -0.6 \end{bmatrix}$, $B = \begin{bmatrix} 0 \\ 0 \\ 1 \end{bmatrix}$, $g(x,t) = 5.6sign(x_1(t))$.

According to Remark 3, we construct the master–slave systems as:
Master chaotic system:

$$\dot{x}_m(t) = Ax_m(t) + Bf(x_m, t) \tag{32}$$

Slave chaotic system:

$$\dot{x}_s(t) = Ax_s(t) + B(f(x_s(t), t) + \Delta f(x_s(t), t) + u(t) + \Delta u(t)) + B_\omega \omega(t) \tag{33}$$

Moreover, the matched and mismatched disturbances and uncertain uncertainty in control input are given as

$$\Delta f(x_s(t), t) = 0.2x_{s1}(t) + 0.2\cos(6t), \Delta u(t) = 0.3\sin(x_{s1}(t))u(t), \omega(t) = 0.3\sin(8t) \tag{34}$$

We can easily check that the pair (A, B) is controllable.

From (34), we have $\alpha_1 = 0.2, \alpha_2 = 0.2, \alpha_u = 0.3, \alpha_\omega = 0.3$.

According to Step 2 in Remark 3, we can easily select the gain matrix $K = [4.8 \ 10 \ 5.4]$ such that $\lambda_1 = -1, \lambda_2 = -2, \lambda_3 = -3$ to result in a stable sliding mode. And we can design the switching function $S(t)$ with $\sigma = \begin{bmatrix} 0 & 0 & 1 \end{bmatrix}$ as

$$S(t) = \begin{bmatrix} 0 & 0 & 1 \end{bmatrix} e(t) + \int_0^t \begin{bmatrix} 6 & 11 & 6 \end{bmatrix} e(\tau) d\tau \tag{35}$$

And eigenvector matrix P corresponding to eigenvalues of matrix $\widetilde{A}$ is obtained as

$$P = \begin{bmatrix} -0.5774 & 0.2182 & -0.1048 \\ 0.5774 & -0.4364 & 0.3145 \\ -0.5774 & 0.8729 & -0.9435 \end{bmatrix}$$

In the following, according to the matrix B_ω, we split it into mismatched and matched conditions to discuss.

(i)　Mismatched condition:

　　Now we examine the mismatched case by assuming $B_\omega = \begin{bmatrix} 0.2 & 0.5 & 0.6 \end{bmatrix}^T$. The proposed SMC $u(t)$ is utilized to synchronize the master–slave systems given in (32) and (33). To reduce the chatting phenomenon, we replace the sign function with the saturation function (29). Therefore, the sliding mode control with saturation function is given as

$$u(t) = -\xi\psi(t)sat(S(t)), \ \xi = 1.5 > (1 - \alpha_u)^{-1} \tag{36}$$

$$sat(S(t)) = \frac{S(t)}{|S(t)| + 0.01}$$

$$\psi(t) = \|5.6(sign(x_{s1}(t)) - sign(x_{m1}(t)) + \begin{bmatrix} 4.8 & 10 & 5.4 \end{bmatrix} e(t)\| \tag{37}$$

$$+ 0.2\|x_s(t)\| + 0.8$$

　　The simulation results with the initial values of $\begin{bmatrix} x_{m1}(0) & x_{m2}(0) & x_{m3}(0) \end{bmatrix}^T = \begin{bmatrix} 3 & -3 & 6 \end{bmatrix}^T$ and $\begin{bmatrix} x_{s1}(0) & x_{s2}(0) & x_{s3}(0) \end{bmatrix}^T = \begin{bmatrix} 5 & -5 & 4 \end{bmatrix}^T$. The upper bound $|e_i(t)|$ of every synchronization error state can be estimated according to (15) and obtained as $\rho_1 \leq 0.26$, $\rho_2 \leq 0.06$ and $\rho_3 \leq 0.15$. Then, the synchronization error responses with estimated bounds, the time response of SMC controller and the sliding surface are presented in Figures 2 and 3, respectively.
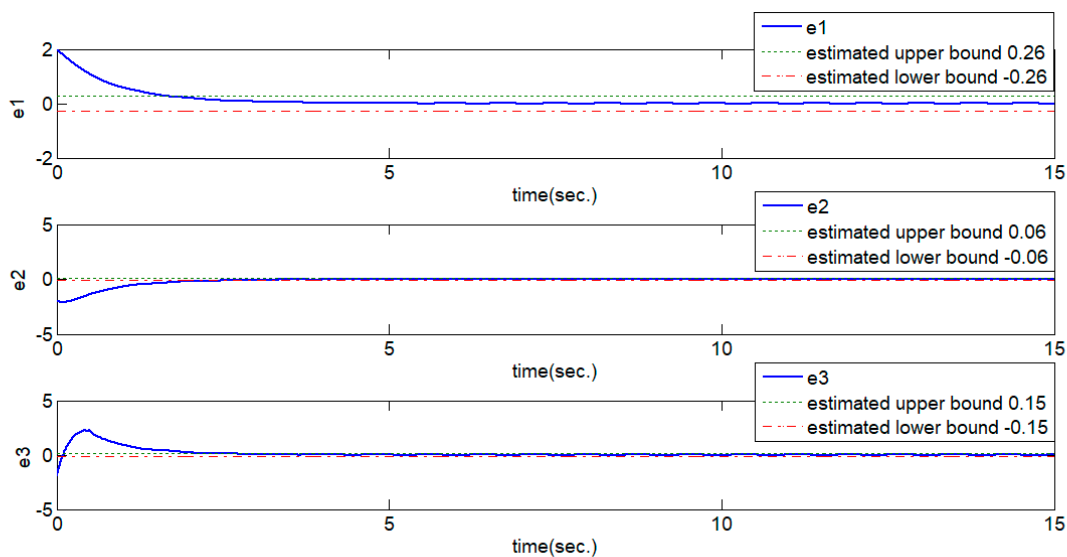
Figure 2. The synchronization error responses with estimated bounds (mismatched condition).
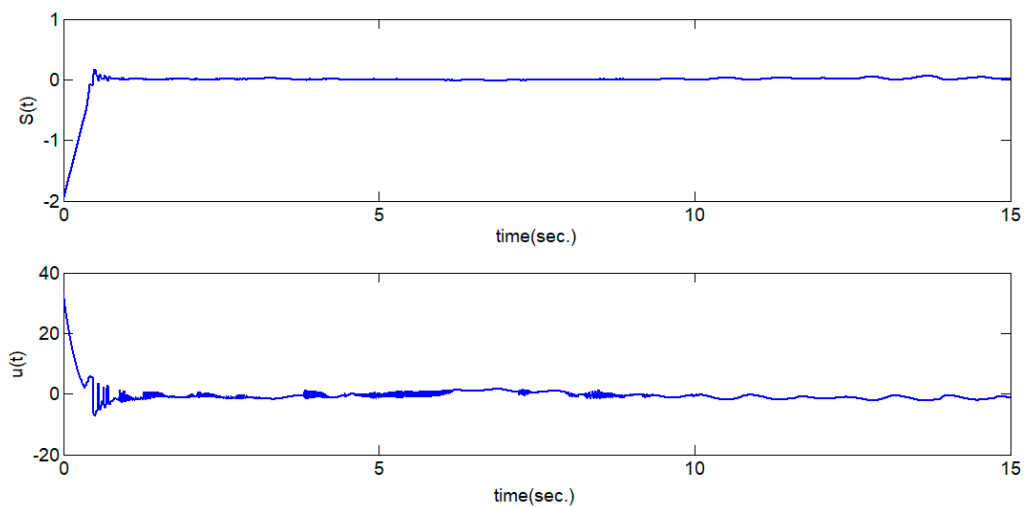
Figure 3. The time responses of the proposed SMC controller and sliding surface.

(ii)　Matched condition:

We continue to simulate the matched case by assuming $B_\omega = \begin{bmatrix} 0 & 0 & 0.5 \end{bmatrix}^T$. In the simulation, we also use the same conditions as those in case (i). The synchronization error trajectories for every $e_i(t)$ are presented in Figure 4. Observing Figure 4, the synchronization errors with matched disturbances exactly converge to zero as concluded in Remark 1.
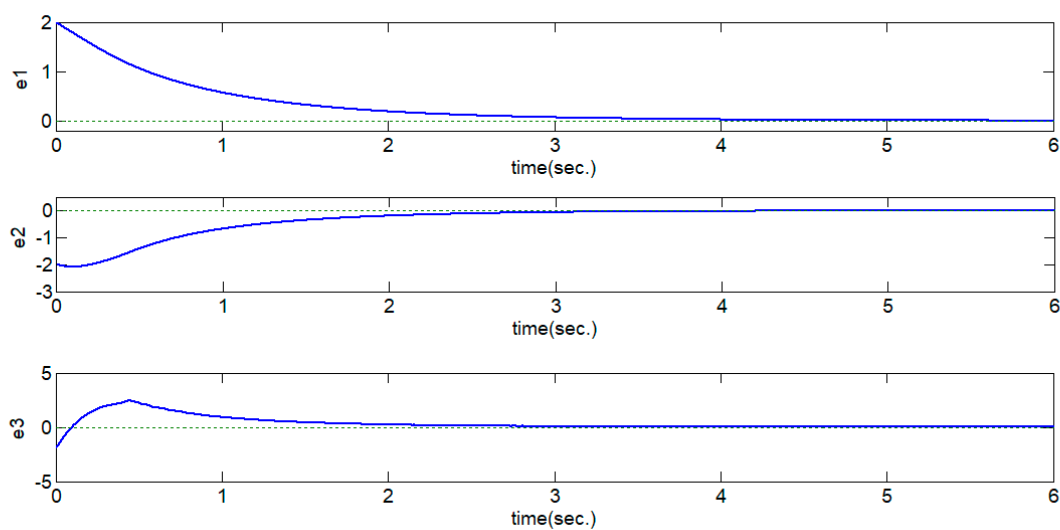
Figure 4. The synchronization error responses (matched condition).

Example 2. *A four-dimensional generalized Lorenz–Stenflo system [25] is considered as follows*

$$\dot{x}_1(t) = a(x_2(t) - x_1(t)) + sx_3(t)$$
$$\dot{x}_2(t) = cx_1(t) - dx_2(t) - x_1(t)x_4(t)$$
$$\dot{x}_3(t) = -x_1(t) - rx_3(t)$$
$$\dot{x}_4(t) = x_1(t)x_2(t) - bx_4(t)$$

(38)

where $x_i, i = 1, 2, 3, 4$, are the state variables and a, b, c, r, s, d are positive parameters.

System (38) exhibits hyperchaotic strange attractors, as shown in Figure 5 with $a = 19.42, b = 1.91, c = 29.45, r = 2.86, s = 0.23, d = 9.64$.
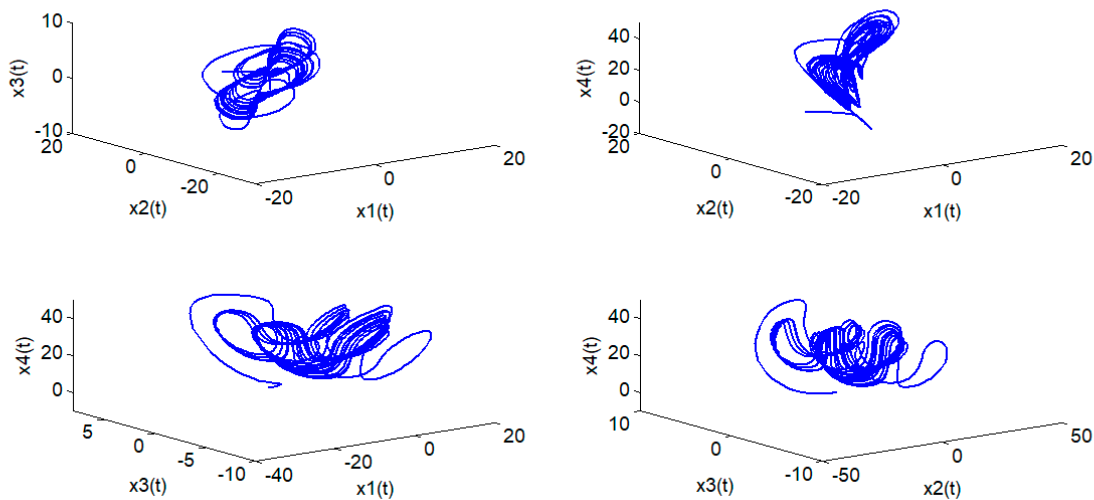
Figure 5. Chaotic strange attractor of generalized Lorenz–Stenflo system.

System (38) can be also rewritten by the general form as

$$\dot{x}(t) = Ax(t) + Bf(x,t) \tag{39}$$

where $A = \begin{bmatrix} -a & a & s & 0 \\ c & -d & 0 & 0 \\ -1 & 0 & -r & 0 \\ 0 & 0 & 0 & -b \end{bmatrix}$, $B = \begin{bmatrix} 0 & 0 \\ 1 & 0 \\ 0 & 0 \\ 0 & 1 \end{bmatrix}$, $f(x,t) = \begin{bmatrix} -x_1(t)x_4(t) \\ x_1(t)x_2(t) \end{bmatrix}$.

We can easily check that (A, B) is controllable with $a = 19.42, b = 1.91, c = 29.45,$ $r = 2.86, s = 0.23, d = 9.64$.

According to Remark 3, we construct the master–slave systems as

Master chaotic system:

$$\dot{x}_m(t) = Ax_m(t) + Bf(x_m, t) \tag{40}$$

Slave chaotic system:

$$\dot{x}_s(t) = Ax_s(t) + B(f(x_s(t), t) + \Delta f(x_s(t), t) + u(t) + \Delta u(t)) + B_\omega \omega(t) \tag{41}$$

In addition, for simulation, the following terms are given as

$$\Delta f(x_s(t), t) = \begin{bmatrix} 0.2\sin(2t)x_{s1}(t) \\ 0.3x_{s2}(t) + 0.2\cos(3t) \end{bmatrix}, \Delta u(t) = \begin{bmatrix} 0.1\sin(t)\cos(3t)u_1(t) \\ 0.2\sin(4t)u_2(t) \end{bmatrix}$$

$$, \omega(t) = \begin{bmatrix} 0.4\sin(8t) & 0.2|\sin(2t)| \end{bmatrix}^T \tag{42}$$

From (42), we have $\alpha_1 = 0.3, \alpha_2 = 0.2, \alpha_u = 0.2, \alpha_\omega = 0.4$.

According to Step 2 in Remark 3, we can obtain the gain matrix

$K = \begin{bmatrix} 38.2330 & -9.5100 & -6.5180 & 0 \\ 0 & 0 & 0 & 3.0900 \end{bmatrix}$ such that $\lambda_1 = -6, \lambda_2 = -4, \lambda_3 = -3, \lambda_4 = -5$ to result in a stable sliding mode. We can also design the switching function $S(t)$ with

$\sigma = \begin{bmatrix} 0 & 1 & 0 & 0 \\ 0 & 0 & 0 & 1 \end{bmatrix}$ as

$$S(t) = \begin{bmatrix} 0 & 1 & 0 & 0 \\ 0 & 0 & 0 & 1 \end{bmatrix} e(t) - \int_0^t \left(\begin{bmatrix} -8.730 & 6.6500 & 6.5180 & 0 \\ 0 & 0 & 0 & -5 \end{bmatrix} e(\tau) \right) d\tau \tag{43}$$

And eigenvector matrix corresponding to eigenvalues of matrix $\widetilde{A}$ is obtained as

$$P = \begin{bmatrix} 0.8463 & -0.8140 & 0.7970 & 0 \\ 0.5120 & -0.5392 & 0.5311 & 0 \\ 0.1467 & -0.2159 & 0.2877 & 0 \\ 0 & 0 & 0 & 1 \end{bmatrix}$$

(i)   Mismatched condition:

Now we check the mismatched case by assuming

$$B_\omega = \begin{bmatrix} 0.3 & 0 \\ 0 & 0.4 \\ 0 & 0.3 \\ 0.2 & 0.1 \end{bmatrix}$$

In order to reduce the chattering, we also use the saturation function (29) to replace the discontinuous sign function. Therefore, $u(t)$ with continuous saturation function can be obtained as

$$u(t) = -\xi \psi(t) sat(S(t)), \ \xi = 1.5 > (1 - \alpha_u)^{-1} \tag{44}$$

$$sat(S(t)) = \begin{bmatrix} \frac{s_1(t)}{|s_1(t)|+0.05} & \frac{s_2(t)}{|s_2(t)|+0.05} \end{bmatrix}^T$$

$$\psi(t) = \left\| \begin{bmatrix} -x_{s1}(t)x_{s4}(t) + x_{m1}(t)x_{m4}(t) \\ x_{s1}(t)x_{s2}(t) - x_{m1}(t)x_{m2}(t) \end{bmatrix} + \begin{bmatrix} -171.1936 & -28.8164 & 0 \\ 0 & 0 & -29.8030 \end{bmatrix} e(t) \right\| \tag{45}$$

$$+0.3\|x_s(t)\| + 0.3664$$

The simulation results are obtained with the initial values of $[x_{m1}(0) \ x_{m2}(0) \ x_{m3}(0) \ x_{m4}(0)] = \begin{bmatrix} -6 & 2 & 2 & 0 \end{bmatrix}$; $\begin{bmatrix} x_{s1}(0) & x_{s2}(0) & x_{s3}(0) & x_{s4}(0) \end{bmatrix} = \begin{bmatrix} -2 & 1 & 3 & 1 \end{bmatrix}$. As described above, the bounds of every synchronization error state $|e_i(t)|$ can be predicted as $\rho_1 \leq 0.1042$, $\rho_2 \leq 0.0713$, $\rho_3 \leq 0.0699$ and $\rho_4 = 0$. Then, the synchronization error responses with predicted bounds, the time response of SMC controller and the sliding surface are presented in Figures 6 and 7, respectively.
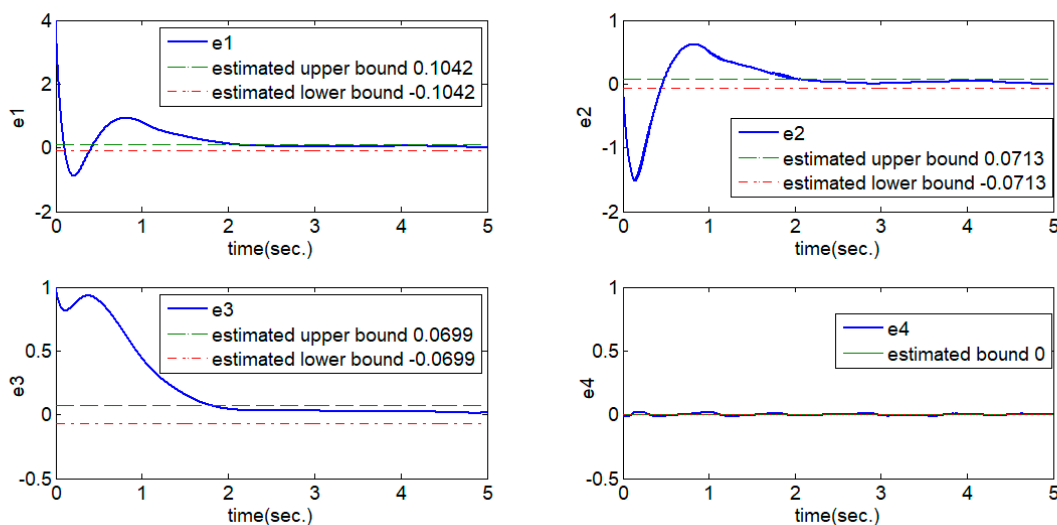
Figure 6. The synchronization error responses with estimated bounds (mismatched condition).
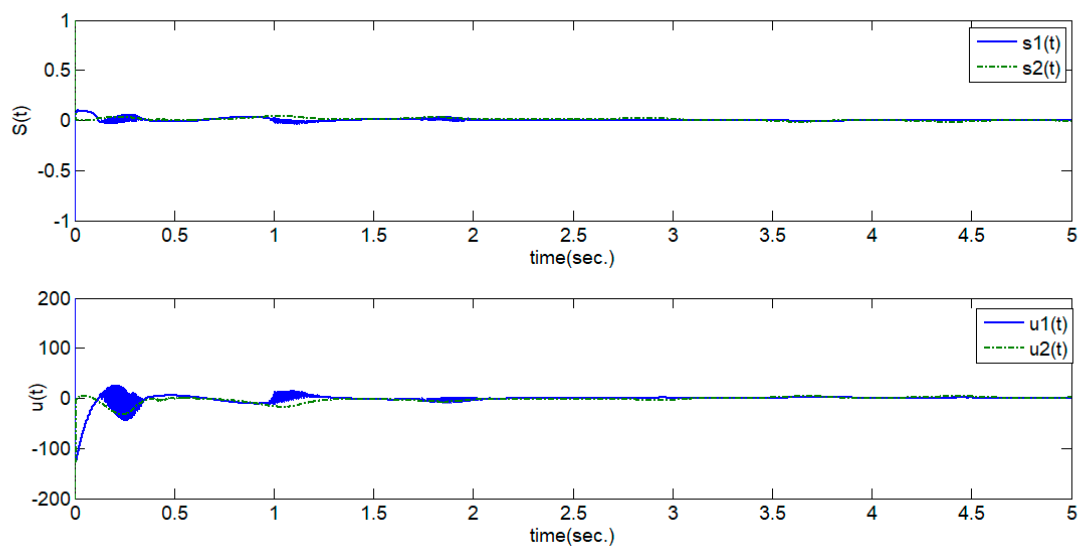
Figure 7. The time responses of the proposed SMC controller and the sliding surface.

(ii)   Matched condition:

Now we continue to study the matched case. The matrix B_ω is given as

$$B_\omega = \begin{bmatrix} 0 & 0 \\ 0.3 & 0 \\ 0 & 0 \\ 0 & 0.3 \end{bmatrix}$$

In the simulation, we use the same conditions as those in case (i) except the disturbance matrix B_w. Then, the synchronization error trajectories of every $e_i(t)$ are presented in Figure 8. Observing Figure 8, the synchronization error under matched disturbances can converge to zero as discussed.
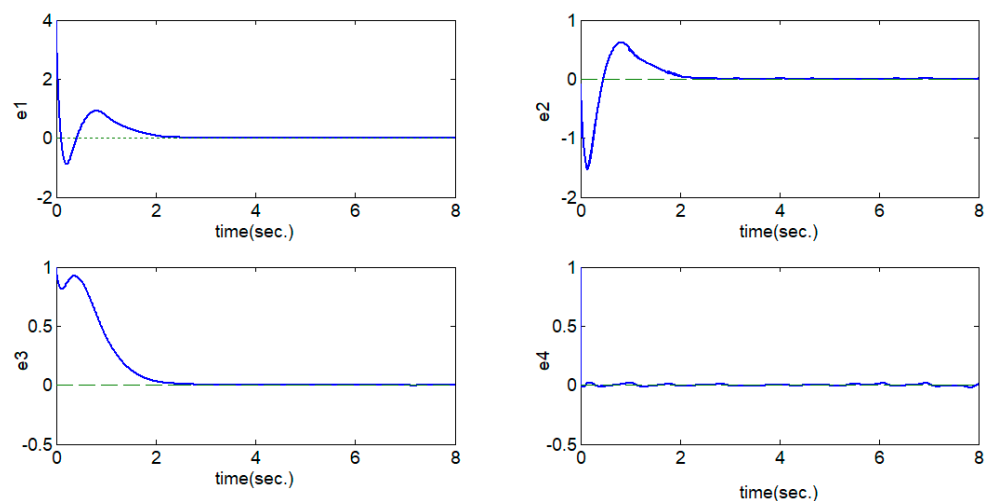
Figure 8. The synchronization error responses (matched condition).

Obviously, according to the simulation results illustrated in Examples 1 and 2, it reveals that the presented robust SMC controller can not only robustly suppress the synchronization errors for matched disturbances, but also predict the synchronization error bounds for mismatched disturbances. The chattering is also reduced by the saturation function. However, a slight influence due to the replacement of the sign function by the saturation function can be observed, but the results are acceptable.

6. Conclusions

A robust chaos synchronization control design for chaotic systems with matched/mismatched disturbances and uncertainty in the input is proposed in this paper. A robust SMC scheme is presented to achieve chaos synchronization even under the influence of matched/mismatched disturbances and nonlinear uncertainty of inputs. The introduced PI type switching surface makes the controlled synchronization error in the sliding manifold easy to analyze. The proposed SMC has great potential in synchronizing uncertain master–slave systems even with mismatched uncertainties as well as input nonlinearity. Moreover, as for the mismatched disturbances, the synchronization errors can also be robustly suppressed to predictable bounds. The design procedure for robust chaos synchronization has been systematized and the numerical simulation results have demonstrated the robustness and validity of the proposed chaos suppression controller.

Author Contributions: All authors contributed to the paper Formal analysis, C.-H.L.; Project administration, J.-J.Y.; Software, C.-H.L.; Writing—original draft, G.-H.H.; Writing—review & editing, J.-J.Y. All authors have read and agreed to the published version of the manuscript.

Institutional Review Board Statement: Not applicable.

Informed Consent Statement: Not applicable.

Data Availability Statement: No new data were created or analyzed in this study. Data sharing is not applicable to this article.

Conflicts of Interest: The authors declare no conflict of interest.

References

1. Sheikhan, M.; Shahnazi, R.; Garoucy, S. Synchronization of general chaotic systems using neural controllers with application to secure communication. *Neural Comput. Appl.* **2011**, *22*, 361–373. [CrossRef]
2. Hoz, M.Z.D.; Acho, L.; Vidal, Y. A modified Chua chaotic oscillator and its application to secure com-munications. *Appl. Math. Comput.* **2014**, *247*, 712–722.
3. Liao, T.-L.; Wan, P.-Y.; Yan, J. Design of Synchronized Large-Scale Chaos Random Number Generators and Its Application to Secure Communication. *Appl. Sci.* **2019**, *9*, 185. [CrossRef]
4. Han, Q.-L. On Designing Time-Varying Delay Feedback Controllers for Master–Slave Synchronization of Lur'e Systems. *IEEE Trans. Circuits Syst. I Regul. Pap.* **2007**, *54*, 1573–1583. [CrossRef]
5. Dadras, S.; Momeni, H. Adaptive sliding mode control of chaotic dynamical systems with application to synchronization. *Math. Comput. Simul.* **2010**, *80*, 2245–2257. [CrossRef]
6. Liu, H.; Wang, H.; Cao, J.; Alsaedi, A.; Hayat, T. Composite learning adaptive sliding mode control of fractional-order nonlinear systems with actuator faults. *J. Frankl. Inst.* **2019**, *356*, 9580–9599. [CrossRef]
7. Lin, T.-C.; Lee, T.-Y. Chaos Synchronization of Uncertain Fractional-Order Chaotic Systems with Time Delay Based on Adaptive Fuzzy Sliding Mode Control. *IEEE Trans. Fuzzy Syst.* **2011**, *19*, 623–635. [CrossRef]
8. Ding, K.; Han, Q.-L. Master-slave synchronization criteria for chaotic hindmarsh-rose neurons using linear feedback control. *Complexity* **2016**, *21*, 319–327. [CrossRef]
9. Bouzeriba, A.; Boulkroune, A.; Bouden, T. Fuzzy adaptive synchronization of uncertain fractional-order chaotic systems. *Int. J. Mach. Learn. Cybern.* **2015**, *7*, 893–908. [CrossRef]
10. Jeong, S.; Ji, D.; Park, J.H.; Won, S. Adaptive synchronization for uncertain chaotic neural networks with mixed time delays using fuzzy disturbance observer. *Appl. Math. Comput.* **2013**, *219*, 5984–5995. [CrossRef]
11. Kuo, C.-L. Design of a fuzzy sliding-mode synchronization controller for two different chaos systems. *Comput. Math. Appl.* **2011**, *61*, 2090–2095. [CrossRef]
12. Lee, S.M.; Ji, D.H.; Park, J.H.; Won, S.C. H∞ synchronization of chaotic systems via dynamic feedback approach. *Phys. Lett. A* **2008**, *372*, 4905–4912. [CrossRef]
13. Qin, Z.; Wang, J.L.; Huang, Y.L.; Ren, S.Y. Synchronization and H∞ synchronization of multi-weighted complex delayed dynamical networks with fxed and switching topologies. *J. Frankl. Inst.* **2017**, *354*, 7119–7138. [CrossRef]
14. Adloo, H.; Roopaei, M. Review article on adaptive synchronization of chaotic systems with unknown parameters. *Nonlinear Dyn.* **2010**, *65*, 141–159. [CrossRef]
15. Liu, B.; Li, J.-P.; Zheng, W. Synchronization and Adaptive Anti-Synchronization Control for Lorenz Systems under Channel Noise with Applications. *Asian J. Control.* **2012**, *15*, 919–929. [CrossRef]

16. Zhang, H.; Mengb, D.; Wang, J.; Lu, G. Synchronization of uncertain chaotic systems via fuzzy-regulated adaptive optimal control approach. *Int. J. Syst. Sci.* **2020**, *51*, 473–487. [CrossRef]
17. Yang, C.-H.; Wang, K.-C.; Wu, L.; Wen, R. State Synchronization for a Class of n-Dimensional Nonlinear Systems with Sector Input Nonlinearity via Adaptive Two-Stage Sliding Mode Control. *Math. Probl. Eng.* **2020**, *2020*, 1–11. [CrossRef]
18. Aghababa, M.P.; Aghababa, H.P. A general nonlinear adaptive control scheme for finite-time synchro-nization of chaotic systems with uncertain parameters and nonlinear inputs. *Nonlinear Dyn.* **2012**, *69*, 1903–1914. [CrossRef]
19. Yang, C.-C.; Lin, C.-L. Adaptive sliding mode control for chaotic synchronization of oscillator with input nonlinearity. *J. Vib. Control.* **2013**, *21*, 601–610. [CrossRef]
20. Wang, C.-C.; Yau, H.-T. Nonlinear dynamic analysis and sliding mode control for a gyroscope system. *Nonlinear Dyn.* **2010**, *66*, 53–65. [CrossRef]
21. Utkin, V. Variable Structure Systems with Sliding Modes: Survey Paper. *IEEE Trans Auto. Control* **1977**, *22*, 212–222. [CrossRef]
22. Deeborah, H.H.; Andrew, M.G.; William, G.M. *Calculus Single and Multivariable 4th Edition with Study Guide*; John & Wiley and Sons: Hoboken, NJ, USA, 2005.
23. Yan, J.J.; Chen, C.Y.; Tsai, J.S.H. Hybrid chaos control of continuous-time unified chaotic systems using discrete rippling sliding mode control. *Nonlinear Anal. Hybrid Syst.* **2016**, *22*, 276–283. [CrossRef]
24. Almeida, D.I.R.; Álvarez, J.; Barajas, J.G.; Barajas-Ramírez, J.G. Robust synchronization of Sprott circuits using sliding mode control. *Chaos Solitons Fractals* **2006**, *30*, 11–18. [CrossRef]
25. Chen, Y.-M.; Liang, H.-H. Zero-zero-Hopf bifurcation and ultimate bound estimation of a generalized Lorenz-Stenflo hyperchaotic system. *Math. Methods Appl. Sci.* **2017**, *40*, 3424–3432. [CrossRef]